Projections of temperature extremes based on preferred CMIP5 models: a case study in the Kaidu-Kongqi River basin in Northwest China

CHEN Li[1], XU Changchun[1,2*], LI Xiaofei[1]

[1] MOE Key Laboratory of Oasis Ecology, College of Resource and Environment Sciences, Xinjiang University, Urumqi 830000, China;
[2] School of Civil Engineering and Environmental Science, University of Oklahoma, Norman OK 73072, USA

Abstract: The extreme temperature has more outstanding impact on ecology and water resources in arid regions than the average temperature. Using the downscaled daily temperature data from 21 Coupled Model Inter-comparison Project (CMIP) models of NASA Earth Exchange Global Daily Downscaled Projections (NEX-GDDP) and the observation data, this paper analyzed the changes in temporal and spatiotemporal variation of temperature extremes, i.e., the maximum temperature (Tmax) and minimum temperature (Tmin), in the Kaidu-Kongqi River basin in Northwest China over the period 2020–2050 based on the evaluation of preferred Multi-Model Ensemble (MME). Results showed that the Partial Least Square ensemble mean participated by Preferred Models (PM-PLS) was better representing the temporal change and spatial distribution of temperature extremes during 1961–2005 and was chosen to project the future change. In 2020–2050, the increasing rate of Tmax (Tmin) under RCP (Representative Concentration Pathway) 8.5 will be 2.0 (1.6) times that under RCP4.5, and that of Tmin will be larger than that of Tmax under each corresponding RCP. Tmin will keep contributing more to global warming than Tmax. The spatial distribution characteristics of Tmax and Tmin under the two RCPs will overall the same; but compared to the baseline period (1986–2005), the increments of Tmax and Tmin in plain area will be larger than those in mountainous area. With the emission concentration increased, however, the response of Tmax in mountainous area will be more sensitive than that in plain area, and that of Tmin will be equivalently sensitive in mountainous area and plain area. The impacts induced by Tmin will be universal and far-reaching. Results of spatiotemporal variation of temperature extremes indicate that large increases in the magnitude of warming in the basin may occur in the future. The projections can provide the scientific basis for water and land plan management and disaster prevention and mitigation in the inland river basin.

Keywords: temperature extremes; multi-model ensemble; RCP; projection; Kaidu-Kongqi River basin

1 Introduction

Temperature plays a key role in climate system. Scientific projection of future temperature change and quantitative assessment of uncertainties of temperature change are not only conducive to the prediction of future climate change, but also significant in formulating policies to cope with climate

*Corresponding author: XU Changchun (E-mail: xcc0110@163.com)
Received 2020-09-22; revised 2021-04-22; accepted 2021-04-27

change (IPCC, 2014; Qin, 2014). In the future, climate warming will further accelerate the water circulation of river basins and change the spatial and temporal distribution of water resources (Chen et al., 2017; Yu et al., 2019). The rising temperature has substantial impacts on agriculture, people's daily lives and socioeconomic development (Barriopedro et al., 2011; Wu and Yan, 2013; Guan et al., 2015). Compared with the average temperature, the impact of extreme temperature on ecology and water resources in arid regions is more outstanding (Yao, 1995; Rosenzweig et al., 2001; Keellings and Waylen, 2012; Ye et al., 2013; Huang et al., 2016; Yu and Sun, 2019). Therefore, studying the characteristics of temperature extremes especially in the arid inland river basin with serious water shortage problem is crucial to local agricultural economic development, water resources distribution and ecological civilization construction.

As an important tool for climate simulation and projection, Global Climate Models (GCMs) have been developed rapidly in recent years (Li et al., 2012; Xu and Xu, 2012a, b; Yao et al., 2012; Chen and Sun, 2013; Wang et al., 2018; Li et al., 2020). The Coupled Model Inter-comparison Project (CMIP) driven by the World Climate Research Program (WCRP) has strongly promoted the development of climate models. In phase 5 of CMIP (CMIP5) new scenarios characterized by RCPs (Representative Concentration Pathways) are adopted, including RCP2.6, RCP4.5, RCP6.0 and RCP8.5. RCPs are a series of integrated concentration and emission scenarios, which are used as input parameters of climate change projection model under the influence of human activities in the 21st century. RCP8.5 will cause the largest magnitude of temperature rise; RCP4.5 is a climate scenario under government intervention, and it is the only emission scenario of cultivated land reduction. In view that the research focus on the temperature extremes, we chose the RCP4.5 and RCP8.5. Lots of studies have evaluated the performance of the CMIP5 models in simulating climatic variability (Hu et al., 2014; Chen et al., 2019). Although the GCMs have remarkable developments, the spatial resolution of them is still limited, and the simulations and projections have much uncertainties and there might be biases associated with dataset, which can further propagate into model results (Chen et al., 2012; Su et al. 2016; Sun et al., 2016). Studies showed that MME (Multi-Model Ensemble) could reduce the uncertainty of future climate projection (Almazroui et al., 2016, 2017a, b). For one thing, the simulation results of MME were closer to observations than most single models; for another, MME by the weighted ensemble method could reduce the uncertainty of estimation. Other studies also pointed out that preferred models outperformed general models in simulation capacity, and PM-PLS (Partial Least Square ensemble mean participated by Preferred Models) had better effect in projection (Xu et al., 2007; Raisanen and Ylhaisi, 2011; Jiang and Wu, 2013; Jiang et al., 2017; Zhang et al., 2017).

High resolution data can be obtained by appropriate downscaled methods for simulation and projection research (Wang et al., 2017; Yang et al., 2017; Raghavan et al., 2018). Raghavan et al. (2018) simulated and evaluated the future climate variation of Southeast Asia with statistical downscaled data and concluded that the NEX-GDDP (NASA Earth Exchange Global Daily Downscaled Projections) data were in good consistency with the observation data. How is the NEX-GDDP used in China, especially in less gauged Northwest China? What data can we use to verify the reliability of NEX-GDDP? The CN05.1 grid dataset developed and maintained by Chinese scientists are supposed to be accurate and reliable because they are interpolated from more than 2400 weather stations and more strictly constrained by surface observations (Xu et al., 2009; Wu and Gao, 2013). In this study, we used CN05.1 to evaluate the accuracy of NEX-GDDP data.

The Kaidu-Kongqi River basin is an inland river basin in the arid region of Northwest China. It is very sensitive to climate change and the signals of global warming have long been found there (Shi et al., 2002). However, it hasn't been known quite clearly what the future climate there will be. Although a few studies have been done to explore it, there was little detailed research about temperature extremes in the basin (He et al., 2018; Li et al., 2019a, b). High-resolution future climate information, including mean condition and extreme condition, is appealed to help scientific research and policy making. This paper takes the Kaidu-Kongqi River basin as the study area and adopts CN05.1 and NEX-GDDP data to simulate and analyze the future temperature extremes, i.e., Tmax (maximum temperature) and Tmin (minimum temperature), in the basin. Firstly, we selected

the models with strong simulation ability in simulating air temperature of the basin from 21 models of NEX-GDDP as preferred models and form the MME. Secondly, we simulated and evaluated the selected single models and MME in temporal and spatial variation based on the historical data. Thirdly, we analyzed the future temperature extremes change in the study area by using the preferred MME (i.e., Partial Least Squares regression non-equal weighted ensemble mean). The objective of this study is to validate the applicability of NEX-GDDP dataset in the study area and to provide a projection of temperature extremes, expecting to help basin managers in water, land and agricultural resources planning and management.

2 Data and methods

2.1 Study area

The Kaidu-Kongqi River basin is located on the southern slope of Tianshan Mountains, Xinjiang, Northwest China (Fig. 1). It has a typical temperate continental arid climate characterized by drought and sparse rain, strong evapotranspiration, large temperature difference during day and night, abundant light and heat. The terrain slopes from northwest to southeast, with the elevation gradually decreasing from 4294 to 767 m.

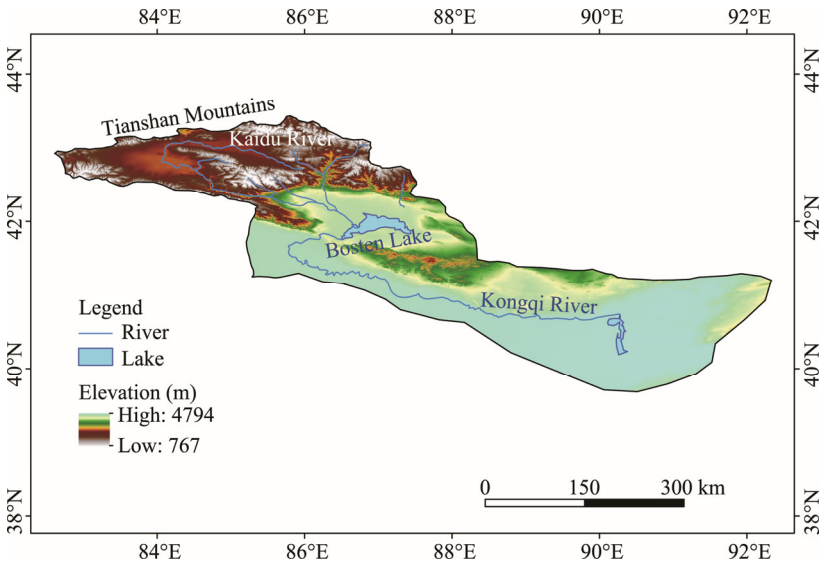

Fig. 1 Sketch map of the Kaidu-Kongqi River basin

2.2 Data

2.2.1 Observation data

The observation data is from CN05.1 dataset (Xu et al., 2009; Wu and Gao, 2013), which includes a series of precipitation, mean temperature, Tmax and Tmin dataset at daily scale with spatial resolution of 0.25 deg×0.25 deg (25 km by 25 km). It is established by anomaly approximation method based on the measured data from more than 2400 weather stations in China. In this paper, the Tmax and Tmin data were used. The period is from 1961 to 2005.

2.2.2 Simulation data

The NEX-GDDP dataset (https://cds.nccs.nasa.gov/nex-gddp/) includes downscaled projections for RCP4.5 and RCP8.5 from the 21 models (Table 1) and scenarios for which daily scenarios were produced and distributed under CMIP5. Each of the climate projections includes daily Tmax, Tmin and precipitation for the period 1950–2100. The spatial resolution of the dataset is 0.25 deg×0.25 deg. This study used the daily Tmax and Tmin. The historical data from 1961 to 2005 was used for simulation evaluation, and the projected data from 2020 to 2050 was used to analyze the temperature extremes.

Table 1 List of 21 GCMs (Global Climate Models) used in NEX-GDDP (NASA Earth Exchange Global Daily Downscaled Projections)

Model name/Country		
ACCESS1-0/Australia	CSIRO-MK3-6-0/Australia	MIROC-ESM/Japan
BCC-CSM1-1/China	GFDL-CM3/USA	MIROC-ESM-CHEM/Japan
BNU-ESM/China	GFDL-ESM2G/USA	MIROC5/Japan
CanESM2/Canada	GFDL-ESM2M/USA	MPI-ESM-LR/Germany
CCSM4/USA	INMCM4/Russia	MPI-ESM-MR/Germany
CESM1-BGC/USA	IPSL-CM5A-LR/France	MRI-CGCM3/Japan
CNRM-CM5/France	IPSL-CM5A-MR/France	NorESM1-M/Norway

2.3 Historical climate simulation performance metric

To facilitate validation of the GCMs against the observational data, we simply averaged the temperature values to define the regionally averaged monthly and annual time series and spatial patterns of GCM simulations and observations. The annual Tmax and Tmin were calculated as the deviations from the climatology during the period 1961–2005. To quantify the agreement between observations and model simulations, we constructed Taylor diagrams (Taylor 2001), for which we calculated the correlation coefficients, STD (standard deviations) and RMSE (root mean square errors) between the CMIP5 models' datasets and the observational datasets. We calculated the trends using linear trend estimation. Partial least squares ensemble mean was employed to calculate and solve the situation where the projection results are unsatisfactory due to the multi-collinearity among independent variables, making the information more in-depth and richer (Zhi et al., 2016).

3 Results and discussion

3.1 Evaluation of model performance

3.1.1 Preferred model selection

In this paper, the two ensemble means participated by all models are called EE (equal-weight ensemble mean) and PLS (Partial Least Square), respectively, according to the two different ways of determining weights. The two ensemble means participated by preferred models are called PM-EE (equal-weight ensemble mean participated by preferred models) and PM-PLS, respectively. The screening criteria for preferred models in this paper are as follows:

- The simulated air temperature of the models shows an increasing trend, passing the significance test of 1%;
- The correlation coefficient between the simulated and observed annual mean Tmax and Tmin time series passes the significance test of 1%.

According to the standards above, 4 and 17 preferred models are selected for Tmax and Tmin, respectively (Table 2). The models, BCC-CSM1-1 and MPI-ESM-LR, have the closest linear trend values to the observations with the increasing rates (both 0.17℃/decade) slightly higher than that of observed (0.16℃/decade), but they didn't pass the significance test. The correlation coefficients of the models, ACCESS1-0, CSIRO-MK3-6-0, GFDL-ESM2M and NorESM1-M, are higher than others and both the linear trend and correlation coefficient have passed significance test. Therefore, these four models are used in the preferred MME, ie., PM-EE and PM-PLS for the Tmax. The performance of the models in simulating Tmin is obviously better than that in simulating Tmax either in trend size or in correlation coefficient. Besides the selected 4 models, the other 13 models, i.e., BCC-CSM1-1, BNU-ESM, CanESM2, CCSM4, CESM1-BGC, CNRM-CM5, GFDL-CM3, GFDL-ESM2G, IPSL-CM5A-LR, IPSL-CM5A-MR, MIROC5, MIROC-ESM, MPI-ESM-MR, are used for Tmin.

3.1.2 Simulation evaluation based on Taylor diagram

The agreement between model-simulated and observed temperature is further evaluated through the Taylor diagrams. Figure 2 shows the results for the climatology difference of different models

in the entire historical period. Based on a comparison of the Taylor diagrams for temporal variability, most of the models have the similar ability to simulate the temperature time series, and different models show some differences. Most of the models can simulate the variability of Tmax well, with a RMSE>0.61 and a close match to CN05.1 observations. The difference between the simulation results of Tmin is the correlation coefficient, ranging from 0.42 to 0.69, which indicates that some models had better simulation ability. In general, CSIRO-MK3-6-0, GFDL-ESM2M and NorESM1-M perform somewhat better for both Tmax and Tmin.

For the MMEs, the temperature simulation results are close to the observed values, the correlation coefficient of Tmax is between 0.47 and 0.61, the RMSE is 0.44–0.48, and the STD is larger than the observed value, ranging from 0.31 to 0.44; the correlation coefficient of Tmin is between 0.80 and 0.83, the RMSE is 0.42–0.46, the STD range is the same as Tmax. The results of Tmax have similar characteristics, and that is large deviation from the observed values. In general, the simulation performance of MME is better than that of single models.

Table 2 Simulated linear trends and the correlation coefficients between the simulated and observed temperature series for the period of 1961–2005

No.	Model name	Maximum temperature			Minimum temperature		
		Linear trend	Correlation coefficient	Preferred model	Linear trend	Correlation coefficient	Preferred model
1	ACCESS1-0	0.30**	0.42**	√	0.31**	0.58**	√
2	BCC-CSM1-1	0.17**	0.23	\	0.20**	0.38**	√
3	BNU-ESM	0.29**	0.23	\	0.36**	0.51**	√
4	CanESM2	0.22**	0.32*	\	0.29**	0.63**	√
5	CCSM4	0.28**	0.29	\	0.32**	0.51**	√
6	CESM1-BGC	0.28**	0.23	\	0.26**	0.49**	√
7	CNRM-CM5	0.11	0.39**	\	0.18**	0.51**	√
8	CSIRO-MK3-6-0	0.13*	0.38**	√	0.21**	0.58**	√
9	GFDL-CM3	0.19**	0.22	\	0.20**	0.45**	√
10	GFDL-ESM2G	0.23**	0.27	\	0.23**	0.48**	√
11	GFDL-ESM2M	0.19**	0.64**	√	0.20**	0.57**	√
12	INMCM4	0.06	0.07	\	0.13*	0.17	\
13	IPSL-CM5A-LR	0.28**	0.30*	\	0.31**	0.59**	√
14	IPSL-CM5A-MR	0.28**	0.26	\	0.29**	0.50**	√
15	MIROC5	0.25**	0.34*	\	0.25**	0.55**	√
16	MIROC-ESM	0.13**	0.16	\	0.14**	0.51**	√
17	MIROC-ESM-CHEM	0.20**	0.03	\	0.24**	0.36*	\
18	MPI-ESM-LR	0.17**	0.01	\	0.17**	0.23	\
19	MPI-ESM-MR	0.25**	0.30	\	0.26**	0.49**	√
20	MRI-CGCM3	0.10	–0.04	\	0.12	0.06	\
21	NorESM1-M	0.27**	0.41**	√	0.25**	0.57**	√
22	EE	0.21**	0.47**		0.23**	0.80**	
23	PLS	0.21**	0.51**		0.25**	0.82**	
24	PM-EE	0.22**	0.62**		0.25**	0.82**	
25	PM-PLS	0.23**	0.61**		0.26**	0.83**	
	CN05.1	0.16*			0.41**		

Note: ** and * represent the results passed the significance test with confidence level of 1% and 5%, respectively; "√" means the model is preferred and selected; "\" means the model is not selected as preferred one.

3.2 Simulation and evaluation in temporal variation

It can be seen from Table 2 and Figure 3 that the Tmax and Tmin in the basin have shown a significant increasing trend in the past 45 a, and all the single models and MMEs indicate this change trend.

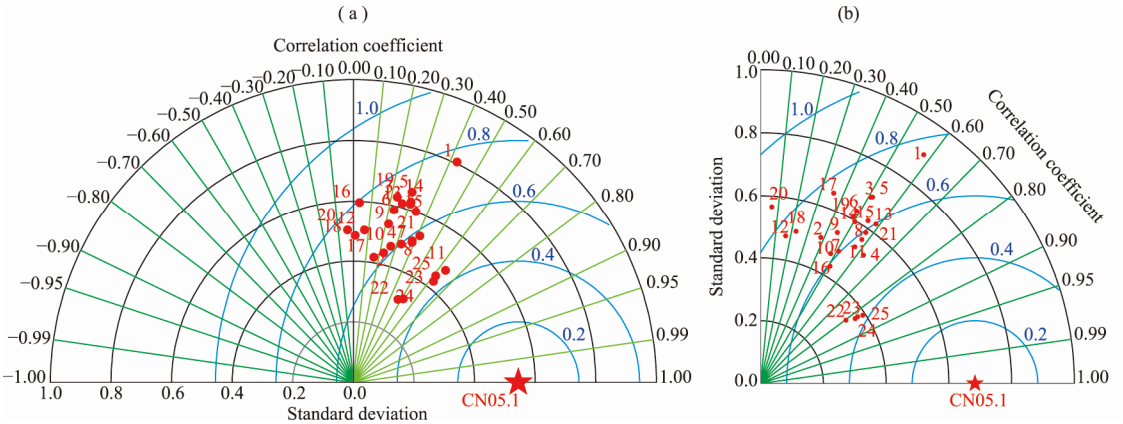

Fig. 2 Taylor diagram for temporal variability of Tmax (maximum temperature) (a) and Tmin (minimum temperature) (b) in the Kaidu-Kongqi River basin between the observations and simulations for the period of 1961–2005. Each number representing a model ID was listed in Table 2.

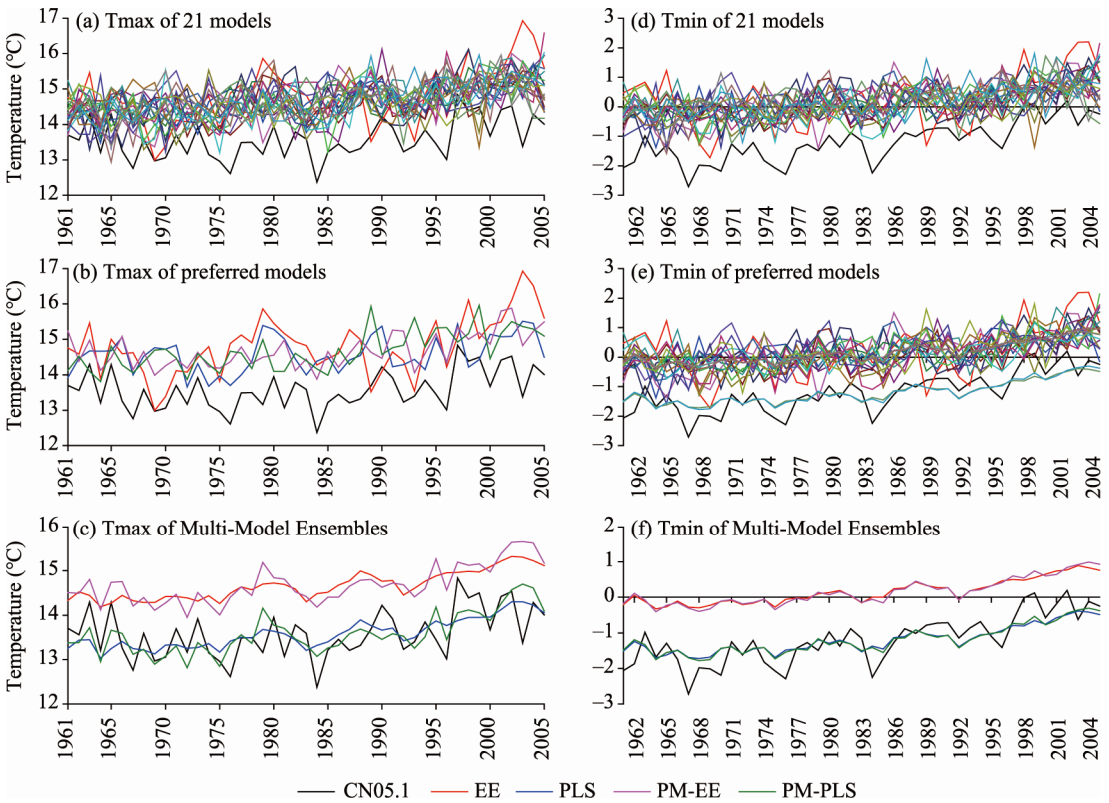

Fig. 3 Simulated Tmax and Tmin in the Kaidu-Kongqi River basin for the period 1961–2005 from CN05.1 observations denoted by black line and from CMIP5 models denoted by colored lines. CN05.1, observation; EE equal-weight ensemble mean; PLS, Partial Least Square; PM-EE, equal-weight ensemble mean participated by preferred models; PM-PLS, Partial Least Square ensemble mean participated by Preferred Models.

In terms of Tmax, the simulated increasing rates of the most models and the four MMEs (0.17°C–0.30°C/decade) are higher than that observed (0.16°C/decade) (Table 2; Fig. 3). That is to say, the most models overestimate the historical change in Tmax (Fig. 3a). The main reason is that the most models cannot simulate the downtrend before the mid-1980s but instead replace it with an uptrend or short downtrend, which magnifies the overall growth trend. The selected preferred models cannot overcome this, either (Fig. 3b), but after applying the MME mean method, the results are improved greatly (Fig. 3c). The four MMEs show very similar variations from 1961 to 2005. However, EE and

PM-EE overestimate Tmax significantly. PLS and PM-PLS are close to the observation curve. In comparison, PM-PLS outperforms PLS in simulating the peaks and valleys better.

As to the Tmin in the basin, the increasing rates of all the models (0.12℃/decade–0.36℃/decade) including single models and MMEs are lower than that of observed (0.41℃/decade) (Table 2). In other words, all the models underestimate the historical change of Tmin in increasing rate. However, the simulated values are greater than the observed values (Fig. 3d). That is because there is a big gap between the early simulation values and the observed values, resulting in the whole gently increasing rate. Thus, the increasing rate alone cannot tell whether the temperature are overestimated or underestimated. Compared to Tmax, Tmin has larger increasing rates (Table 2), meaning Tmin increased stronger than Tmax, which are consistent with the results of most studies (Zhao at al., 2014; Sun et al., 2016; Shang et al., 2018). Similarly, EE and PM-EE overestimate Tmin significantly. Both PLS and PM-PLS are close to the observation curve, but they cannot well depict the change in peaks and valleys due to the smooth effect caused by too much preferred models participated in.

3.3 Simulation and evaluation in spatial variation

In Figure 4, according to the observed results (Fig. 4a), the annual mean Tmax is between –0.9℃ and 21.5℃, showing a gradually increasing trend from northwest to southeast with the altitude decreasing. All the models can capture the spatial distribution characteristics. For the

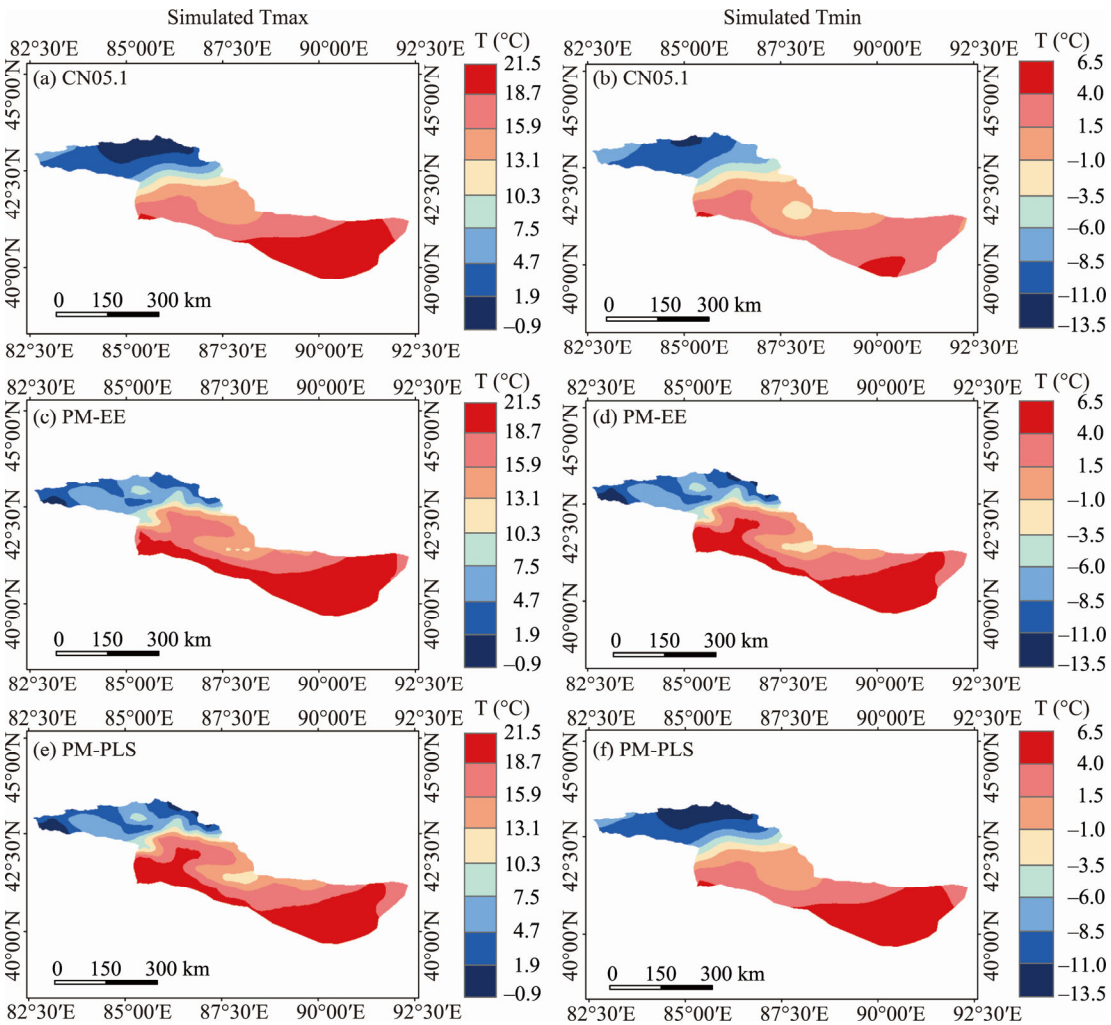

Fig. 4 Simulated Tmax and Tmin in the Kaidu-Kongqi River basin during 1961–2005 for spatial change. T, temperature.

MME, both PM-EE and PM-PLS can well reproduce the distribution range of the Tmax (Fig. 4c and e), but PM-PLS has a closer result of spatial distribution pattern to that of observation.

The annual average Tmin changes from –13.5℃ to 6.5℃ (Fig. 4b), which can be shown in most of the models, and it shows the similar spatial distribution characteristics as that of the Tmax. Specially, a small area located in the middle of the basin is found to be colder than the adjacent area, which could be the result of cold island effect exerted by the Bosten Lake (Fig. 1). As to the MME, PM-EE can simulate the overall characteristics of Tmin, but it performs poorly in representing the specific distribution in plain and mountainous area. For example, large area of high values in the south does not tell the true characteristics of the Bosten Lake around (Fig. 4d). In contrast, PM-PLS has a relatively better simulation result with the spatial correlation coefficient approaching to 1.0.

Figure 5 shows the spatial correlation coefficient distribution of Tmax and Tmin between PM-EE, PM-PLS and the observed. Generally, the flatter and simpler the region, the better the simulation effect. High-resolution models can better reflect the steep topographic features of the high-altitude area and eliminate the high deviations that exist, thus improving the simulation capability (Jiang et al., 2016). Based on the spatial simulation results (Fig. 5), we can draw that Tmin has a better simulation performance than Tmax and PM-PLS is better than PM-EE in exhibiting the spatial distribution of temperature extremes.

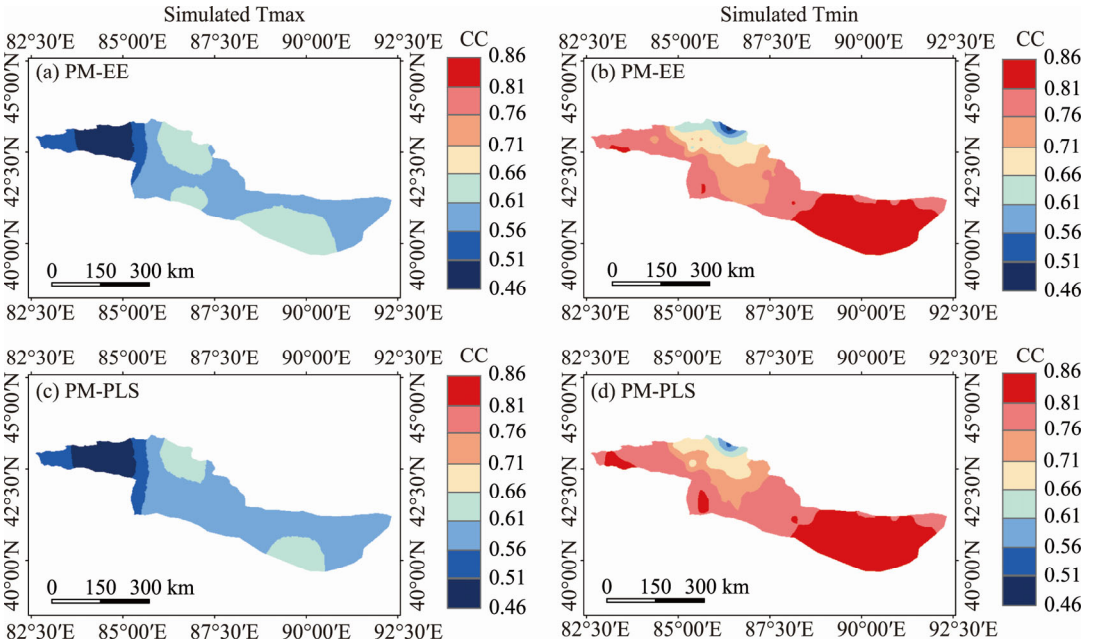

Fig. 5 Spatial correlation coefficient (CC) distribution of Tmax and Tmin in the Kaidu-Kongqi River basin during 1961–2005 between PM-EE and observation (CN05.1) (a, b) and between PM-PLS and CN05.1 (c, d)

3.4 Future temperature projection

3.4.1 Temperature in temporal change

Based on the evaluation results, PM-PLS is adopted to estimate the future change in the temperature extremes of the basin. In Figure 6, it shows that Tmax under RCP4.5 will increase as a whole during 2020–2050 with an increasing rate of 0.24℃/decade (Fig. 6a), higher than that of the historical period (0.16℃/decade) and half of that under RCP8.5 (0.48℃/decade) (Fig. 6c). The fluctuation range (14.5℃–16.5℃) and the annual mean (about 15.5℃) of Tmax under RCP4.5 closely approximate that under RCP8.5, meaning that the large difference in RCPs will not necessarily cause marked difference in the basic characteristics of Tmax in short-term. They differ in two specific aspects. One is the fluctuation period; the former will fluctuate violently after 2030 and the latter will do before 2040. The other is the increasing trend; the former will not increase continuously but jump from one stage to another with no obvious growth within each stage, while

the latter will increase almost continuously.

As for Tmin, the increasing rates under RCP4.5 (Fig. 6b) and RCP8.5 (Fig. 6d) are 0.36℃/decade and 0.56℃/decade, respectively, higher than those of Tmax under the corresponding RCPs, indicating that Tmin will keep contributing more to global warming than Tmax as before. However, the increasing rate of Tmin under RCP4.5 is found lower than that of the historical period (0.41℃/decade). In addition, there will be a ten-year warming hiatus since 2035. All these indicate that the moderate emission scenario can relieve warming to some extent. In contrast, Tmin under RCP8.5 will keep continuous increase and approach to 2.4℃ at the mid-21st century.

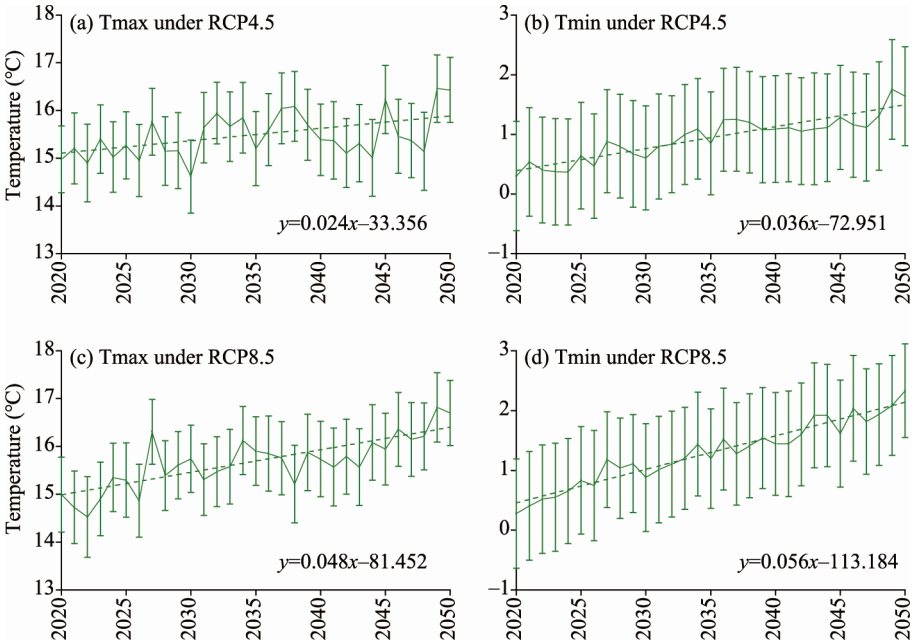

Fig. 6 Projected Tmax and Tmin under RCP (Representative Concentration Pathway) 4.5 and RCP8.5, respectively, in the Kaidu-Kongqi River basin during 2020–2050. The dashed lines denote the corresponding linear trends and the symbols on the line denote the STD (standard deviation).

3.4.2 Analysis of temperature in spatial change

Tmax under RCP4.5 and RCP8.5 reveals the same spatial distribution characteristics that temperature is low at the northwest part ranging from 0.9℃ to 9.3℃ and high at the southeast part hovering from 14.9℃ to 23.3℃ (Fig. 7a and b). There is no obvious difference between the two scenarios in short-term. Compared to the baseline period, however, they behave differently. The increment of temperature is 1.1℃–1.7℃ for mountainous area and 1.6℃–2.0℃ for plain area under RCP4.5 (Fig. 7c), and it is 1.2℃–2.1℃ and 1.6℃–2.1℃, respectively, under RCP8.5 (Fig. 7d). Tmax will increase under both RCPs in the whole basin. In comparison, the increment of temperature is larger in mountainous area and lower in plain area with the emission concentration increased. That is to say, Tmax in the mountainous area is more susceptible to be affected by the increased emission concentration.

In terms of Tmin, it shows almost the same spatial distribution characteristics as Tmax (Fig. 8a and b). Similarly, there is no difference between the two RCPs. Tmin ranges from –9.4℃ to –3.4℃ at the northwest mountainous area and from 0.6℃ to 6.6℃ at the southeast plain area. Compared to the baseline period, the increment of temperature is 1.0℃–1.8℃ for mountainous area and 1.4℃–2.2℃ for plain area under RCP4.5 (Fig. 8c), and it is 1.3℃–1.9℃ and 1.6℃–2.2℃, respectively, under RCP8.5 (Fig. 8d). Tmin will increase under both RCPs in the whole basin. The increments of temperature are large in both mountainous area and plain area with the emission concentration increased. So, the impact of increased emission concentration on Tmin is universal in the basin.

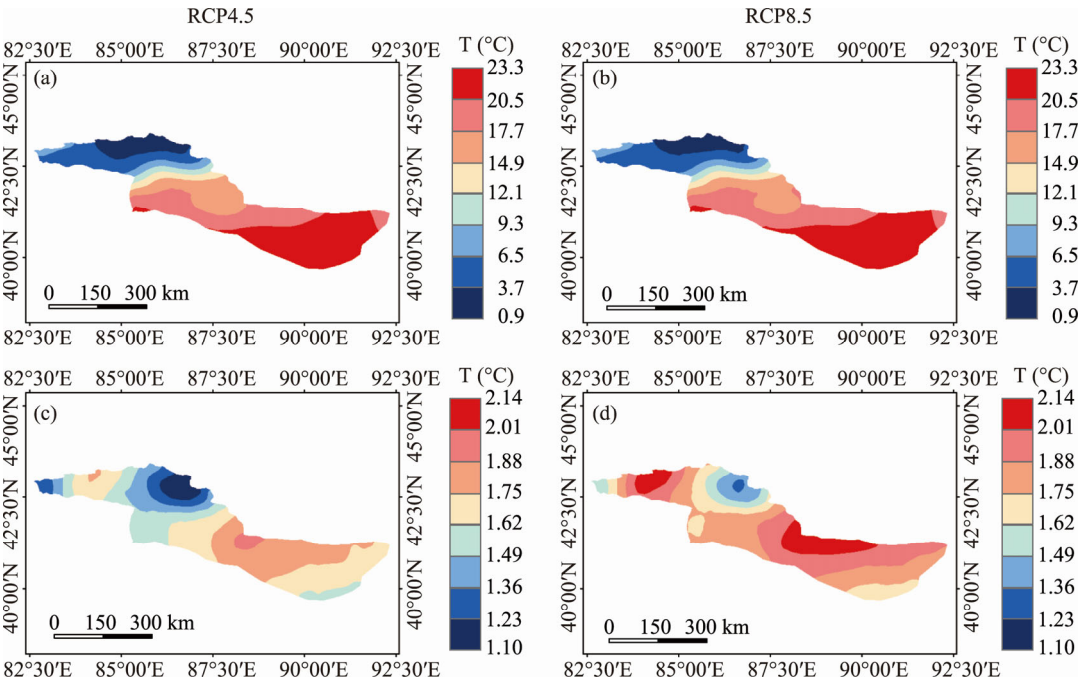

Fig. 7 Projected Tmax under RCP4.5 and RCP8.5 in 2020–2050 (a, b) and the changes relative to the baseline period 1986–2005 (c, d)

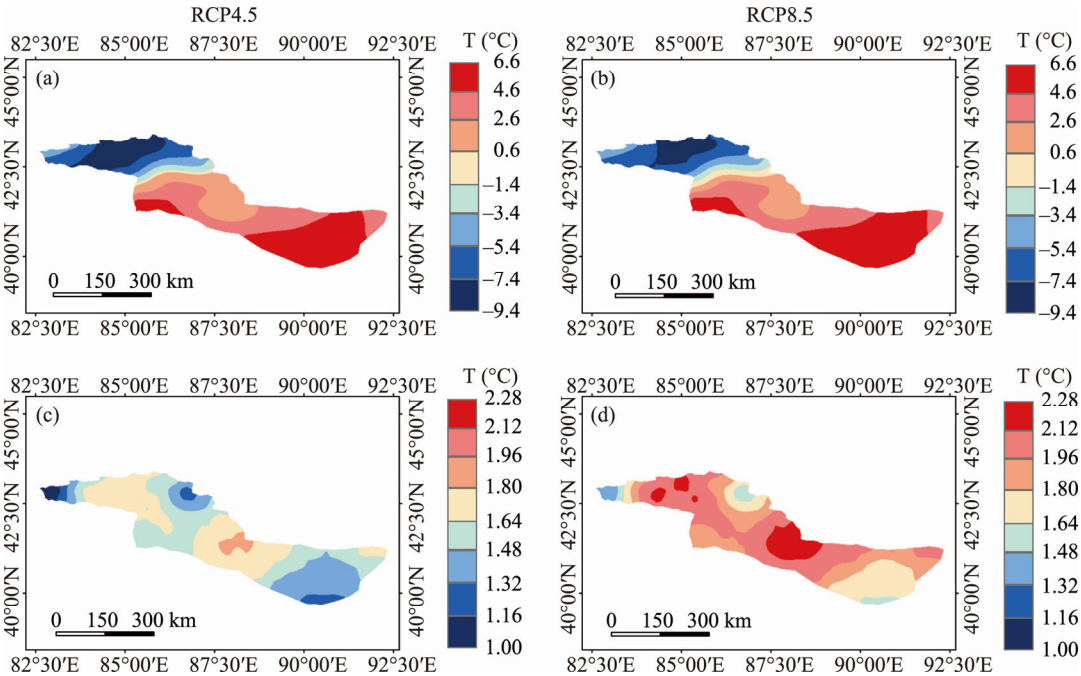

Fig. 8 Projected Tmin under RCP4.5 and RCP8.5 in 2020–2050 (a, b) and the changes relative to the baseline period 1986–2005 (c, d)

4 Conclusions

The present paper analyzed the temperature extremes of the Kaidu-Konqi River basin during 2020–2050. Both the Tmax and Tmin under RCP4.5 and RCP8.5 will increase in the future. The increasing rates of Tmin will be larger than those of Tmax under each corresponding RCP. The

spatial distribution characteristics of Tmax and Tmin under RCP4.5 and RCP8.5 will overall the same in short-term, that is, the temperature in northwest is low and in southeast is high. The increment of Tmax and Tmin will be larger in plain area than that in mountainous area.

Temperature extremes are the important indicators of global warming, and analyzing them is helpful for us to know climate change. In this paper, the observed dataset verified the accuracy of selected models and the reliability of ensemble mean. However, the MMEs used in this paper were produced by only two simple methods, i.e., PM-EE, and PM-PLS. So far there is no good way to solve the problem of scientifically determine the distribution of weights. It needs our further study. Currently, CMIP6 has updated a number of climate model data, it is recommended to use the latest data for further research. In addition, the study mainly used the statistical downscaled data, and its spatial resolution is still coarse, which restricts the accuracy and reliability of simulation and projection. Combined using dynamic and statistical downscaled data will be a try in the future.

Acknowledgements

This research is supported by the National Natural Science Foundation of China (41561023) and China Scholarship Council (201808655036). We are grateful to editors and anonymous reviewers for their helpful comments on improvement of the manuscript.

References

Almazroui M, Saeed F, Islam M N, et al. 2016. Assessing the robustness and uncertainties of projected changes in temperature and precipitation in AR4 global climate models over the Arabian Peninsula. Atmospheric Research, 182: 163–175.

Almazroui M, Nazrul I M, Saeed S, et al. 2017a. Assessment of uncertainties in projected temperature and precipitation over the Arabian Peninsula using three categories of Cmip5 multimodel ensembles. Earth Systems and Environment, 23(2017), doi: 10.1007/s41748-017-0027-5.

Almazroui M, Tayeb O, Mashat A S, et al. 2017b. Saudi-KAU coupled global climate model: description and performance. Earth Systems and Environment, 7(2017), doi: 10.1007/s41748-017-0009-7.

Barriopedro D, Fischer E M, Luterbacher J, et al. 2011. The hot summer of 2010: redrawing the temperature record map of Europe. Science, 332(6026): 220–224.

Chen H P, Sun J Q. 2013. Projected change in East Asian summer monsoon precipitation under RCP scenario. Meteorology and Atmospheric Physics, 121(1–2): 55–77.

Chen S F, Wu R G, Song L Y, et al. 2019. Present-day status and future projection of spring Eurasian surface air temperature in CMIP5 model simulations. Climate Dynamics, 52: 5431–5449.

Chen W L, Jiang Z H, Huang Q. 2012. Projection and simulation of climate extremes over the Yangtze and Huaihe River Basins based on a Statistical Downscaling Model. Transactions of Atmospheric Sciences, 35(5): 578–590. (in Chinese)

Chen Y N, Li Z, Fang G H, et al. 2017. Impact of climate change on water resources in the Tianshan Mountians, Central Asia. Acta Geographica Sinica, 72(1): 18–26. (in Chinese)

Guan Y H, Zhang X C, Zheng F L, et al. 2015. Trends and variability of daily temperature extremes during 1960–2012 in the Yangtze River Basin, China. Global and Planetary Change, 124: 79–94.

He D D, Xu C C, Liu J C. 2018. Future climate scenarios projection in the Kaidu River basin based on ASD statistical down-scaling model. Pearl River, 39(9): 25–32. (in Chinese)

Hu Q, Jiang D B, Fan G Z. 2014. Evaluation of CMIP5 models over the Qinghai–Tibetan Plateau. Chinese Journal of Atmospheric Sciences, 38(5): 924−938. (in Chinese)

Huang J P, Yu H P, Guan X D, et al. 2016. Accelerated dryland expansion under climate change. Nature Climate Change, 6(2): 166–171.

IPCC (Intergovernmental Panel on Climate Change). 2014. Climate Change 2014: impacts, adaptation, and vulnerability. Part A. Global and Sectoral Aspects. Contribution of working groups I, II and III to the Fifth Assessment Report of the Intergovernmental Panel on Climate Change. Cambridge: Cambridge University Press.

Jiang D B, Tian Z P, Lang X M. 2016. Reliability of climate models for China through the IPCC Third to Fifth Assessment Reports. International Journal of Climatology, 36(3): 1114–1133.

Jiang S, Jiang Z H, Li W, et al. 2017. Evaluation of the extreme temperature and its trend in China simulated by CMIP5 models. Climate Change Research, 13(1): 11–24. (in Chinese)

Jiang Y M, Wu H M. 2013. Simulation Capabilities of 20 CMIP5 Models for Annual Mean Air Temperatures in Central Asia. Progressus Inquisitiones DE Mutatione Climatis, 9(2): 110–116. (in Chinese)

Keellings D, Waylen P. 2012. The stochastic properties of high daily maximum temperatures applying crossing theory to modeling high-temperature event variables. Theoretical and Applied Climatology, 108: 579–590.

Li H L, Wang H J, Yin Y Z. 2012. Interdecadal variation of the West African summer monsoon during 1979–2010 and associated variability. Climate Dynamics, 39(12): 2883–2894.

Li X F, Xu C C, Li L, et al. 2019a. Projection of future climate change in the Kaidu-Kongqi River Basin in the 21st Century. Arid Zone Research, 36(3): 556–566. (in Chinese)

Li X F, Xu C C, Li L, et al. 2019b. Evaluation of air temperature of the typical river basin in desert area of Northwest China by the CMIP5 models: A case of the Kaidu-Kongqi River Basin. Resources Science, 41(6): 1141–1153. (in Chinese)

Li X M, Simonovic S P, Li L H, et al. 2020. Performance and uncertainty analysis of a short-term climate reconstruction based on multi-source data in the Tianshan Mountains region, China. Journal of Arid Land, 12(3): 374–396.

Qin D H. 2014. Climate change science and sustainable development. Progress in Geography, 33(7): 874–883. (in Chinese)

Raghavan S V, Hur J, Liong S. 2018. Evaluations of NASA NEX-GDDP data over Southeast Asia: present and future climates. Climatic Change, 148: 503–518.

Raisanen J, Ylhaisi J S. 2011. How much should climate model output be smoothed in space? Journal of Climate, 24(3): 867–880.

Rosenzweig C, Iglesias A, Yang X B, et al. 2001. Climate change and extreme weather events; implications for food production, plant diseases, and pests. Global Change and Human Health, 2: 90–104.

Shang S S, Lian L Z, Ma T, et al. 2018. Spatiotemporal variation of temperature and precipitation in Northwest China in recent 54 years. Arid Zone Research, 35(1): 68–76. (in Chinese)

Shi Y F, Shen Y P, Hu R J. 2002. Preliminary study on signal, impact and foreground of climatic shift from warm-dry to warm-humid in Northwest China. Journal of Glaciology and Geocryology, 24(3): 219–226. (in Chinese)

Su B D, Huang J L, Gemmer M, et al. 2016. Statistical downscaling of CMIP5 multi-model ensemble for projected changes of climate in the Indus River Basin. Atmospheric Research, 178–179: 138–149.

Sun Q H, Miao C Y, Duan Q Y. 2016. Extreme climate events and agricultural climate indices in China: CMIP5 model evaluation and projections. International Journal of Climatology, 36(1): 43–61.

Taylor K E. 2001. Summarizing multiple aspects of model performance in a single diagram. Geophysical Research Letters, 106(D7): 7183–7192

Wang L, Guo S L, Hong X J, et al. 2017. Projected hydrologic regime changes in the Poyang Lake Basin due to climate change. Frontiers of Earth Science, 11: 95–113.

Wang M H, Li H L, Sun X T. 2018. Quantitative evaluation on the interannual and interdecadal precipitation variability simulated by six CMIP5 models of China. Meteorological Monthly, 44(5): 634–644. (in Chinese)

Wu D, Yan D H. 2013. Projections of future climate change over Huaihe River basin by multi-model ensembles under SRES scenarios. Journal of Lake Sciences, 25(4): 565–575. (in Chinese)

Wu J, Gao X J. 2013. A gridded daily observation dataset over China region and comparison with the other datasets. Chinese Journal of Geophysics, 56(4): 1102–1111. (in Chinese)

Xu C H, Shen X Y, Xu Y. 2007. An analysis of climate change in East Asia by using the IPCC AR4 simulations. Advances in Climate Change Research, 3(5): 287–292. (in Chinese)

Xu C H, Xu Y. 2012a. The projection of temperature and precipitation over China under RCP scenarios using a CMIP5 multi-model ensemble. Atmospheric and Oceanic Science Letters, 5(6): 527–533.

Xu Y, Gao X J, Shen Y, et al. 2009. A daily temperature dataset over China and its application in validating a RCM simulation. Advances in Atmospheric Sciences, 26(4): 763–772.

Xu Y, Xu C H. 2012b. Preliminary assessment of simulations of climate changes over China by CMIP5 multi-models. Atmospheric and Oceanic Science Letters, 5(6): 47–52.

Yang X L, Zheng W F, Lin C Q. 2017. Prediction of drought in the Yellow River Basin based on statistical downscaling study and SPI. Journal of Hohai University (Natural Sciences), 45(5): 377–383. (in Chinese)

Yao P Z. 1995. The climate features of summer low temperature cold damage in northeast China during recent 40 years. Journal of Catastrophology, 10(1): 51–56. (in Chinese)

Yao Y, Luo Y, Huang J B. 2012. Evaluation and projection of temperature extremes over China based on 8 modeling data from CMIP5. Advances in Climate Change Research, 3(4): 179–185.

Ye L M, Yang G X, van Ranst E, et al. 2013. Time-series modeling and prediction of global monthly absolute temperature for environmental decision making. Advance in Atmospheric Sciences, 30(2): 382–396.

Yu E T, Sun J Q. 2019. Extreme temperature projection over northwestern China based on multiple regional climate models. Transactions of Atmospheric Sciences, 42(1): 46–57. (in Chinese)

Yu Y, Pi Y Y, Yu X, et al. 2019. Climate change, water resources and sustainable development in the arid and semi-arid lands of Central Asia in the past 30 years. Journal of Arid Land, 11(1): 1–14.

Zhang X Z, Li X X, Xu X C, et al. 2017. Ensemble projection of climate change scenarios of China in the 21st century based on the preferred climate models. Acta Geographica Sinica, 72(9): 1555–1568. (in Chinese)

Zhao T B, Chen L, Ma Z G. 2014. Simulation of historical and projected climate change in arid and semiarid areas by CMIP5 models. Chinese Science Bulletin, 59(4): 1148–1163.

Zhi X F, Zhao H, Zhu S P, et al. 2016. Superensemble hindcast of surface air temperature using CMIP5 multimodel data. Transactions of Atmospheric Science, 39(1): 64–71. (in Chinese)